



## Formation Control Algorithms for Multi-UAV Systems with Unstable Topologies and Hybrid Delays

Wu, J., Luo, C., Min, G., & Mcclean, S. (2024). Formation Control Algorithms for Multi-UAV Systems with Unstable Topologies and Hybrid Delays. *IEEE Transactions on Vehicular Technology*, 1-12. Advance online publication. <https://doi.org/10.1109/TVT.2024.3383352>

[Link to publication record in Ulster University Research Portal](#)

**Published in:**  
IEEE Transactions on Vehicular Technology

**Publication Status:**  
Published online: 08/04/2024

**DOI:**  
[10.1109/TVT.2024.3383352](https://doi.org/10.1109/TVT.2024.3383352)

**Document Version**  
Author Accepted version

**General rights**  
Copyright for the publications made accessible via Ulster University's Research Portal is retained by the author(s) and / or other copyright owners and it is a condition of accessing these publications that users recognise and abide by the legal requirements associated with these rights.

**Take down policy**  
The Research Portal is Ulster University's institutional repository that provides access to Ulster's research outputs. Every effort has been made to ensure that content in the Research Portal does not infringe any person's rights, or applicable UK laws. If you discover content in the Research Portal that you believe breaches copyright or violates any law, please contact [pure-support@ulster.ac.uk](mailto:pure-support@ulster.ac.uk).

# Formation Control Algorithms for Multi-UAV Systems with Unstable Topologies and Hybrid Delays

Jia Wu, Chunbo Luo, Geyong Min, Sally McClean

**Abstract**—Multi-UAV systems rely on the communication network to exchange mission-critical data for their coordination and deployment, while communication delays could cause significant challenges to both tasks. The impact of the delays becomes even more severe if the delay, network structure and formation are all time-varying, a common challenge faced by real-world multi-UAV systems. To address this challenge, we consider time-varying delays that exist in multiple channels caused by transmitting information and internal delays that exist in UAVs themselves caused by obtaining and processing their own data. We design an effective distributed formation control protocol for a multi-UAV system to achieve time-varying formation; this protocol is particularly useful for dealing with time-varying multi-UAV network topologies as well. We provide rigorous convergence analysis for different scenarios with or without hybrid delays and obtain sufficient conditions for achieving the time-varying formation. Furthermore, we propose an algorithm for quantifying the maximum delay allowed by the system. Based on the designed formation algorithm, a deployment strategy is proposed to coordinate multi-UAV systems in a practical environment. Numerical analysis and UAV hardware experiments are conducted to evaluate the performance of the theoretical results and investigate the feasibility of generated flight trajectories.

**Index Terms**—Multi-UAV systems, formations, time-varying topologies, hybrid delays, UAV deployment

## I. INTRODUCTION

Unmanned aerial vehicles (UAVs) are gaining increased popularity in civilian applications, due to their versatile capabilities to execute tasks that are often dangerous or difficult for human beings [1]. Many UAV applications have brought significant advantages in terms of improved efficiency and timeliness, such as agriculture [2], searching and rescuing [3] [4], mobile edge computing [5] and delivering [6]. All of these applications require UAVs to be deployed effectively. Furthermore, compared with a single UAV, multi-UAV systems can cooperate to complete more complex tasks and have much improved efficiency and robustness. They have thus attracted wide research interest over the past decades.

Generally, multiple UAVs are coordinated by formation algorithms to fly with a specific geometry and bring key benefits to the overall system, including energy-saving and more stable communication links. Various formation control algorithms have been developed to implement multifarious formations in

different scenarios. For example, Wu et al. [7] and Duan et al. [8] designed consensus-based distributed formation protocols to achieve desired formations. A significant number of studies, e.g. [9]–[12], adapted the leader-follower approaches to control the follower agents' velocities so that they are consistent with the leader's. Some other studies applied the behavioural characteristics of biological groups to the formation of UAV systems to realise autonomy and swarm intelligence [13]–[15]. Despite the success in formation algorithms, the existing formation work usually assumes ideal network communication among the UAVs group for coordination and synchronisation and has not paid sufficient attention to the challenges caused by time-delay in communication and dynamic network structure during formation flight [7]–[10].

Due to the complexity and variability of practical deployment environments, wireless connections among UAVs of a formation group, which are used for sharing key status information (e.g. position and velocity) during formation and tasking, are often unstable because of interference and fading. Therefore, the communication topologies exhibit significant time-varying features. Research efforts (e.g. [16]–[19]) for solving the problem of unstable communication topologies with different constraints assume that the system maintains the jointly connected condition. This condition means that the union graph of the system's communication network topology graph should be connected over a given period of time. It is still difficult to meet in many practical environments. Savino [20] assumed that the topology changes according to Markov jumps with uncertain rates of transitions, which simulates the randomness of the actual channel to some extent. However, this system requires UAVs to obtain their own information and their neighbours' status information through wireless networks and is thus subject to delays. Some other researchers, e.g. [21] and [22], addressed the time-delay problem by assuming all time delays in different wireless channels are invariant. Similar approaches are also adopted in [23] which assumes that time-varying delays of all channels are the same. Liu et al. [24] addressed this problem from a more practical perspective by considering multiple time-varying delays for a first-order multi-agent system including the internal delay that occurs when individuals obtain their own information and designing a convergent control protocol to ensure the stability of the system. Yan et al. [25] studied an event-triggered controller for multi-UAV formation flying with delays, but they only investigated the internal delay of processing signals that is only part of multiple delays.

J. Wu, C. Luo, and G. Min are with the Department of Computer Science, University of Exeter, Exeter, EX4 4QF, U.K. (e-mail: {jw1241, c.luo, g.min}@exeter.ac.uk) (Corresponding author: C. Luo)

Sally McClean is with the School of Computing, Ulster University, Newtownabbey, BT37 0QB, U.K. (e-mail: si.mcclean@ulster.ac.uk)

Most existing algorithms of UAV deployment focus on two problems: which UAVs should be deployed and what the trajectories are to the target points. For example, Sharma et al. [26] modelled the two problems as a decision-making problem. They derived a decision matrix by combining the entropy of the area with the entropy of the UAV. Considering the deployment in UAV-assisted wireless networks for disaster management, Masroor et al. [27] addressed a multi-objective problem of UAV placement, users-UAV connectivity, distance, and cost, in order to maximize the number of users with a minimum number of UAVs. To implement these deployment algorithms in practice, effective control methods are prerequisites to support them. In this paper, the proposed distributed controller can be used to generate feasible trajectories to the target points and help the deployment of UAVs effectively.

This paper models the multi-UAV system as a second-order system and proposes novel formation control algorithms to address the time delay and time-varying network issues critical to multi-UAV systems. Compared with the study [24] that designed a decaying control protocol coefficient for a first-order system to ensure system convergence, the feedback matrix we have designed for the control protocols in the second-order system is fixed and suitable for various situations, which makes it easier to control the system because it does not need to adjust the parameters by itself. [28] adopted a state-feedback control approach to form a desired formation and follow a specified trajectory, where communication delays and disturbances are constrained but the topology has to be fixed. In this paper, we take into account the joint effect of time-varying topologies and delays. Wang et al. [29] also studied the communication delays and switching topology, where the second-order system and the structure of the control protocol are similar to ours. Yan et al. [25] only investigated the internal delay and used a uniform delay to represent all delays. Compared to their work, the communication delay in different channels considered in this paper is time-varying instead of uniform in [25], [29]. Further, we investigate the time-varying internal delay in each UAV caused by internal data acquisition (e.g. GPS data) and processing. Compared to the work [29], [30], our system can allow a larger delay, which is more realistic and can meet the requirements of actual scenarios [31]. Motivated by the above discussions, the main contributions of our work are summarised below:

- We propose effective distributed time-varying formation control protocols and deduce the sufficient conditions for multi-UAV systems to achieve desired and time-varying formations and easy deployment of UAVs.
- We study the multiple delays and dynamic topologies that are close to actual scenarios. With randomly connected or disconnected topologies, we consider not only time-varying delays in different wireless channels but also internal delays caused by data acquisition and processing, and prove the convergence of the proposed algorithm.
- Furthermore, we propose an algorithm for computing the maximum delay allowed by the system, which was not studied by most related work [24], [29], [30].

The remainder of this paper is organized as follows. Sec-

tion 2 presents the key notations and the network model of the multi-UAV system. Section 3 introduces the designed distributed control protocols and presents the corresponding certification processes. In Section 4, simulation and hardware experiments are presented to demonstrate the models and verify the theoretical results. In Section 5, we summarize this paper and discuss some future research directions.

## II. PRELIMINARIES

TABLE I  
THIS TABLE SUMMARIZES THE KEY NOTATIONS.

Notations	Description
$R^n$	$n$ -dimensional vector
$R^{m \times n}$	Matrix with $m$ rows and $n$ columns
$I_n$	Identity matrix with $n$ dimensions
$A_{i,j}$	The $i$ th row and $j$ th column element of matrix $A$
$A^n$	$A^n = \prod_{i=0}^{n-1} A$
$\lambda_i(A)$	The $i$ th eigenvalue of matrix $A$
$\lambda_N$	The maximum eigenvalue of Laplace matrix
$\rho(A)$	The spectral radius of matrix $A$
$\ A\ $	$l_2$ norm of matrix $A$
$\ A\ _\infty$	Infinite norm of matrix $A$
$[\cdot]^T$	Matrix or vector transpose
$\otimes$	Kronecker product
$v_{k,l}$	$v_{k,l} = 1$ , if $k = l$ ; $v_{k,l} = 0$ , otherwise
$\Pi_{k,l}^U$	$\Pi_{k,l}^U = U(k)U(k-1) \dots U(l)$ , if $k \geq l$ ; $\Pi_{k,l}^U = I_n$ , otherwise
$\lceil x \rceil$	A minimum integer greater than $x$

The multi-UAV network topology can be modelled by an undirected graph as  $\mathcal{G} = \{\mathcal{V}, \mathcal{E}, W\}$ , where  $\mathcal{V} = \{1, 2, \dots, N\}$  is the set of vertices with  $N$  being the total number of vertices, and each vertex represents a UAV. The wireless communication links between UAVs are denoted by  $\mathcal{E} = \{(j, i) | i, j \in \mathcal{V}\}$  with  $(j, i)$  being the channel from the  $j$ th UAV to the  $i$ th UAV.  $W = [w_{ij}] \in R^{N \times N}$  is the adjacent matrix of the graph. If a channel  $(j, i)$  exists,  $w_{ij} = 1$ . Otherwise,  $w_{ij} = 0$ . Here we only consider the communication between UAVs, so  $w_{ii} = 0, i = 1, \dots, N$ . In addition,  $w_{ij} = w_{ji}$  for reciprocal channels, modelled as undirected graphs. The degree matrix is denoted by  $D = \text{diag}\{d_1, d_2, \dots, d_N\}$ , where  $d_i = \sum_{j=1}^N w_{ij}$ . Then, we can obtain the Laplacian matrix  $L = D - W$ . Notably, if each channel changes over time, the graph model becomes  $\mathcal{G}(t) = \{\mathcal{V}, \mathcal{E}(t), W(t)\}$ . Then, the Laplacian matrix  $L(t)$  is also time-varying in this case. Table 1 summarizes the key notations.

Focusing on the formation strategy, UAVs are usually treated as particles characterized by their position and velocity, while the other factors of UAVs such as shape and internal structures have less impact and can be simplified in this scenario [32] [33]. Then, according to the kinematic equations of UAVs, the UAVs system is modelled as a second-order discrete-time system as follows

$$\begin{cases} x_i(t+1) = x_i(t) + \sigma v_i(t) \\ v_i(t+1) = v_i(t) + \sigma u_i(t) \end{cases} \quad (1)$$

where  $x_i(t) \in R^n$  measured in metres ( $m$ ) is the position of the  $i$ th UAV with  $t$  being the time steps;  $v_i(t) \in R^n$  is the velocity measured in metres per second ( $m/s$ ) at the  $t$ th steps.  $u_i(t) \in R^m$  measured in metres per second squared ( $m/s^2$ ) is

the formation controller to be designed later, which plays a key role in driving the UAVs to achieve the anticipated formation and can be regarded as accelerated velocity.  $\sigma > 0$  measured in second ( $s$ ) represents the length of a series of time slots.

Eq. (1) can be rewritten into the first-order form by denoting  $\xi_i(t) = [x_i(t), v_i(t)]^T$

$$\xi_i(t+1) = \xi_i(t) + \sigma (A\xi_i(t) + Bu_i(t)) \quad (2)$$

where  $A = I_n \otimes \begin{bmatrix} 0 & 1 \\ 0 & 0 \end{bmatrix}$  and  $B = I_n \otimes \begin{bmatrix} 0 \\ 1 \end{bmatrix}$ . It is equivalent to Eq. (1) but is easier to analyze the convergence.

The anticipated formation of the  $i$ th UAV is denoted by  $f_i(t) = [f_{ix}(t), f_{iv}(t)]^T$ , where  $f_{ix}(t)$  denotes the time-varying formation position and  $f_{iv}(t)$  denotes the time-varying formation velocity. Denote  $h_i(t)$  as the formation trajectory of the  $i$ th UAVs. Because the entire formation is time-varying, each individual has a different trajectory. Moreover, the distance between each individual and the centre of the formation is also time-varying.

**Definition 1.** *The multi-UAV system achieves the time-varying formation if  $h_i(t)$  exists such that  $\lim_{t \rightarrow \infty} (\xi_i(t) - f_i(t) - h_i(t)) = 0, i = 1, \dots, N$  is satisfied.*

### III. PROBLEM FORMULATION AND THEORETICAL RESULTS

#### A. Formation control with time-varying formation and topologies

We first consider a relatively simple case in which the formation and communication topology are time-varying but the time delay in each channel is negligible. The distributed time-varying formation control protocol is designed as follows

$$u_i(t) = K_1 (\xi_i(t) - f_i(t)) + \kappa \cdot \Delta f_{iv}(t) + K_2 \sum_{j=1}^N w_{ij}(t) ((\xi_j(t) - f_j(t)) - (\xi_i(t) - f_i(t))) \quad (3)$$

where  $\Delta f_{iv}(t) = [\Delta f_{iv_1}(t), \dots, \Delta f_{iv_n}(t)]^T$  with  $\Delta f_{iv_n}(t) = f_{iv_n}(t+1) - f_{iv_n}(t)$  and  $\kappa = \frac{1}{\sigma}$ . Note that  $n$  is the dimension. Here we consider three-dimension practical scenarios and  $n = 3$ . Then,  $\kappa \Delta f_{iv}(t)$  represents the acceleration of formation velocity.  $K_1$  and  $K_2$  are important feedback control matrices that affect the system's convergence. The value of  $w_{ij}(t)$  may be 0 or 1 at different times depending on whether the communication channel is disconnected or connected.

In order to further simplify the system model expression, we denote  $\xi(t) = [\xi_1^T(t), \xi_2^T(t), \dots, \xi_N^T(t)]^T$  and the time-varying formation  $F(t) = [f_1^T(t), f_2^T(t), \dots, f_N^T(t)]^T$ . Denote  $\Delta F_v(t) = [\Delta f_{1v}^T(t), \Delta f_{2v}^T(t), \dots, \Delta f_{Nv}^T(t)]^T$ . Then the UAV system (2) can be rewritten as

$$\begin{aligned} & \xi(t+1) \\ &= \xi(t) + (I_N \otimes (\sigma A + \sigma BK_1) - L(t) \otimes \sigma BK_2) \xi(t) \\ & \quad - (I_N \otimes \sigma BK_1 - L(t) \otimes \sigma BK_2) F(t) + (I_N \otimes \sigma \kappa B) \Delta F_v(t) \end{aligned} \quad (4)$$

Let  $e_i(t) = \xi_i(t) - f_i(t) - h_i(t)$  be the formation error. We define  $\delta_i(t) = \xi_i(t) - f_i(t)$ . Let  $\delta(t) = (\delta_1^T(t), \delta_2^T(t), \dots, \delta_N^T(t))^T$

and  $e(t) = (e_1^T(t), e_2^T(t), \dots, e_N^T(t))^T$ . We can obtain the matrix expression of  $\delta(t)$  as follows

$$\begin{aligned} & \delta(t+1) \\ &= \delta(t) + (I_N \otimes (\sigma A + \sigma BK_1) - L(t) \otimes \sigma BK_2) \delta(t) \\ & \quad + (I_N \otimes \sigma A) F(t) - \Delta F(t) + (I_N \otimes \sigma \kappa B) \Delta F_v(t) \end{aligned} \quad (5)$$

where  $\Delta F(t) = F(t+1) - F(t)$ .

The term  $[(I_N \otimes \sigma A) F(t) - \Delta F(t) + (I_N \otimes \sigma \kappa B) \Delta F_v(t)]$  is not affected by the feedback control matrices  $K_1$  and  $K_2$ . To ensure the convergence of the system, we design the time-varying formation that follows the rule  $f_{ix}(t+1) = f_{ix}(t) + \sigma f_{iv}(t)$ . Then, we get  $(I_N \otimes \sigma A) F(t) - \Delta F(t) + (I_N \otimes \sigma \kappa B) \Delta F_v(t) = 0$ .

To simplify the design of  $K_1$  and  $K_2$ . Let  $K = K_2 = -K_1$  and denote the feedback matrix as  $K = I_n \otimes [k_1, k_2]$ . Thus,  $\delta(t)$  is converted into the following equation with the applicable formation

$$\delta(t+1) = (I_N \otimes \tilde{A} - (I_N + L(t)) \otimes \sigma BK) \delta(t) \quad (6)$$

where  $\tilde{A} = I_m + \sigma A$  and  $m$  is the matching dimension. This formula also reflects the importance of the feedback matrix  $K$ . Inappropriate  $K$  will make the system unable to converge.

We introduce the following Lemma 1 to support the analysis of the system.

**Lemma 1.** (*[34]*) *For a graph  $G$ , the maximum eigenvalue of its corresponding Laplacian matrix satisfies*

$$\bar{\lambda}_N(G) \leq \max_{i \in V} \{d_i(t) + m_i(t)\}$$

where  $d_i(t)$  is the degree of node  $i$  and  $m_i(t) = \frac{\sum_{j \in N_i} d_j(t)}{d_i(t)}$  is the average degree.

Then, we elucidate the realizability of time-varying formations based on dynamic network topology through the following theorem.  $\bar{\lambda}_N(\mathcal{G})$  is the upper bound of the eigenvalue of the Laplacian matrix of the graph  $\mathcal{G}$ . In this paper, we have  $\bar{\lambda}_N(\mathcal{G}) = \max\{\bar{\lambda}_N(\mathcal{G}_0), \dots, \bar{\lambda}_N(\mathcal{G}_j)\}$  with  $\mathcal{G}_0, \dots, \mathcal{G}_j$  being the connected sub-graph of  $\mathcal{G}$ . The value of  $\bar{\lambda}_N(\mathcal{G})$  can be estimated based on the basic graph using Lemma 1.

**Theorem 1.** *For multi-UAV systems under the designed formation control protocol (3), if  $0 < k_1, k_2 < 1$  and  $\sigma k_1 < k_2 < \frac{4k_1}{\bar{\lambda}_N(\mathcal{G})+1}$  are satisfied, the time-varying formation  $F(t)$  can be achieved for the multi-UAV system with time-varying network topologies.*

*Proof.* According to the property of the matrix  $I_N + L(t)$ , there exists a unitary matrix  $V^{-1}(t)$  at any time  $t$  such that  $J(t) = V^{-1}(t) (I_N + L(t)) V(t) = \text{diag}\{\lambda_1(t), \dots, \lambda_N(t)\}$  with  $\lambda_i(t) \geq 1, i = 1, \dots, N$ . Note that  $\lambda_i$  is the  $i$ th eigenvalue of the matrix  $I_N + L(t)$ . Denote  $V(t) = [v_1(t), \dots, v_N(t)]$ , where  $v_i(t)$  is the normalized eigenvector corresponding to the eigenvalue  $\lambda_i(t)$  at time  $t$ . Then, we denote  $V^{-1}(t) = [\tilde{v}_1(t); \tilde{v}_2(t); \dots; \tilde{v}_N(t)] = [\tilde{v}_1(t); \tilde{V}(t)]$  with  $\tilde{v}_i$  being the row eigenvector.

Let  $\tilde{h}(t) = (\tilde{v}_1(t) \otimes I_n) \delta(t)$  and  $\tilde{\delta}(t) = (\tilde{V}(t) \otimes I_n) \delta(t)$ . Then, we can define  $\hat{h}(t) = (V(t) \otimes I_n) [\tilde{h}(t), 0]^T$  and  $\hat{\delta}(t) = (V(t) \otimes I_n) [0, \tilde{\delta}(t)]^T$ . Based on their definitions, we have

$$\delta(t) = \hat{h}(t) + \hat{\delta}(t) \quad (7)$$

That is,  $\hat{\delta}(t) = \delta(t) - \hat{h}(t)$ . Let  $h(t) = \hat{h}(t)$  and  $h(t) = (h_1^T(t), h_2^T(t), \dots, h_N^T(t))^T$ . Then, we have  $\hat{\delta}(t)$  that is equivalent to the expression of formation error  $e(t) = \delta(t) - h(t)$ . Provided  $\lim_{t \rightarrow \infty} \|\hat{\delta}(t)\| = 0$  is satisfied, the time-varying formation of multiple UAVs can be realized and  $h(t)$  exists. Because  $\|\hat{\delta}(t)\| = \|\tilde{\delta}(t)\|$ , we only need to consider  $\tilde{\delta}(t)$ . We can write  $\tilde{\delta}(t)$  as

$$\tilde{\delta}(t+1) = (I_N \otimes \tilde{A} - \sigma \tilde{J}(t)BK) \tilde{\delta}(t) \quad (8)$$

where  $\tilde{J}(t) = \text{diag}\{\lambda_2(t), \dots, \lambda_N(t)\}$ . Note that  $\lambda_i$  is the  $i$ th eigenvalue of the matrix  $I_N + L(t)$ .

If we analyze any dimension of the  $i$ th UAV individually, we can obtain

$$\tilde{\delta}_{ij}(t+1) = M \tilde{\delta}_{ij}(t) \quad (9)$$

where  $M = \begin{bmatrix} 1 & \sigma \\ 0 & 1 \end{bmatrix} - \sigma \lambda_i(t) \begin{bmatrix} 0 & 0 \\ k_1 & k_2 \end{bmatrix}$ , which can be regarded as the error system matrix and  $\tilde{\delta}_{ij}$  represents the  $i$ th UAV in the  $j$ th dimension. Next, we need to ensure that the spectral radius of the system matrix  $M$  is less than 1. Then, the Multi-UAV system can be convergent. Therefore, we should guarantee  $\rho(M) < 1$ . Here, we can calculate

$$|\lambda(M)| = \left| 1 - \frac{\sigma \lambda_i(t) k_2}{2} \pm \sqrt{\frac{\sigma^2 \lambda_i^2(t) k_2^2}{4} - \sigma^2 \lambda_i(t) k_1} \right| < 1 \quad (10)$$

To find the appropriate value of  $k_1$  and  $k_2$ , we could set  $k_2 \in [0, 1]$ , and then calculate  $k_1$  based on Eq. (10). Especially, let  $\frac{\sigma^2 \lambda_i^2(t) k_2^2}{4} - \sigma^2 \lambda_i(t) k_1 < 0$  such that  $|\lambda(M)|$  is a complex number and its modulo should be less than 1. Then, we get a conservative solution  $\sigma k_1 < k_2 < \frac{4k_1}{\lambda_i(t)}$  with  $0 < k_1, k_2 < 1$ .

In order to ensure the convergence of each UAV in each dimension, we can estimate the upper bound of the eigenvalue of the time-varying topologies with the help of Lemma 1. Hence, for the graph  $\mathcal{G}$ , the final solutions become  $0 < k_1, k_2 < 1$  and  $\sigma k_1 < k_2 < \frac{4k_1}{\bar{\lambda}_N(\mathcal{G})+1}$ , where  $\bar{\lambda}_N(\mathcal{G}) = \max\{\bar{\lambda}_N(\mathcal{G}_0), \dots, \bar{\lambda}_N(\mathcal{G}_j)\}$  with  $\mathcal{G}_0, \dots, \mathcal{G}_j$  being the connected sub-graph of  $\mathcal{G}$  and  $\bar{\lambda}_N(\mathcal{G})$  being the upper bound of the eigenvalue of the Laplacian matrix of the graph  $\mathcal{G}$ .

Since the eigenvalues of the Laplacian matrix of an undirected graph are non-negative, we can easily estimate the upper bound of its eigenvalues according to Lemma 1. For directed graphs, the eigenvalues of the Laplacian matrix may be negative, so the aforementioned condition of  $k_1$  and  $k_2$  is no longer applicable, but the method can still help with time-varying formation control of multiple drones based on directed graphs. If our directed graph is fixed, then we can directly calculate the maximum eigenvalue and substitute it into inequality (10) for solving; if the directed graph is dynamic, at this time, we need to know the possible forms of the dynamic graph to perform eigenvalue estimation and then get the new condition to achieve time-varying formation.

It is important to further investigate the influence of the control gain  $\sigma$  on the convergence speed of the system. Because the error system matrix  $M$  can be diagonalized and  $l_2$

norm has the property of unitary in-variance, there is a unitary matrix  $R$  such that

$$\begin{aligned} \|\tilde{\delta}_{ij}(t+1)\| &\leq \|RMR^{-1}\| \|\tilde{\delta}_{ij}(t)\| \\ &= \|\text{diag}\{\lambda_1(M), \lambda_2(M)\}\| \|\tilde{\delta}_{ij}(t)\| \end{aligned} \quad (11)$$

Therefore, the spectral radius of  $M$  can reflect the convergence speed of the UAV in the corresponding dimension. In other words, the smaller the eigenvalue  $\lambda_j(M)$ ,  $j = 1, 2$  is, the faster the system converges. We define a convergence rate function of  $\sigma$  as  $f(\sigma) = |\lambda_j(M)|^2 = 1 - \sigma \lambda_j(t) k_2 + \sigma^2 \lambda_j(t) k_1$ . The first derivative of  $f(\sigma)$  is  $f'(\sigma) = -\lambda_j(t) k_2 + 2\sigma \lambda_j(t) k_1$ . Therefore, we can draw a conclusion that if  $2\sigma k_1 < k_2$  is satisfied, the larger  $\sigma$  is, the smaller the value of function  $f(\sigma)$  is. In other words, the system will converge faster with a larger  $\sigma$ . The proof is thus completed.  $\square$

### B. Formation control with time-varying topologies and varying time-delays

This subsection studies the impact of varying delays among different communication channels of a multi-UAV system over time-varying topologies. The time delays include both transmission delays and internal data processing delays. Let  $t_{i,j}$  denote transmission delay from the channel  $i$  to  $j$ , and  $t_{i,i}$  represents internal data processing delay.

**Assumption 1.** We assume the delays in a multi-UAV system are bounded to satisfying

$$0 \leq t_{i,j} \leq t_{m_1}$$

$$0 \leq t_{i,i} \leq t_{m_2}.$$

where  $t_{i,j}$ ,  $t_{i,i}$ ,  $t_{m_1}$  and  $t_{m_2}$  are measured in second (s). Let  $\tau_{i,j} = \lceil \frac{t_{i,j}}{\sigma} \rceil$ ,  $\tau_{i,i} = \lceil \frac{t_{i,i}}{\sigma} \rceil$ . Denote  $\tau_m = \max\{\lceil \frac{t_{m_1}}{\sigma} \rceil, \lceil \frac{t_{m_2}}{\sigma} \rceil\}$ , which indicates the time step of the delay.

If delays are greater than the bounds, the communication link is assumed to be disconnected and the corresponding delayed packets should be dropped, which are common settings in real-world networks.

Considering the joint effect of time-varying topologies and varying time delays, the distributed formation control protocol becomes

$$\begin{aligned} &u_i(t) \\ &= K_1 (\xi_i(t - \tau_{i,i}(t)) - f_i(t)) + \kappa \cdot \Delta f_v(t) \\ &\quad + K_2 \sum_{j=1}^N w_{ij}(t) ((\xi_j(t - \tau_{j,i}(t)) - f_j(t)) - (\xi_i(t - \tau_{i,i}(t)) - f_i(t))) \end{aligned} \quad (12)$$

The delay in each channel is considered in the above protocol (12). The meaning of other parameters is the same as the control protocol without delay.

Let  $\hat{L}_{ij,\tau}$  be the element of a special Laplace matrix  $\hat{L}_\tau$  with  $0 \leq \tau < \tau_m$ , and it satisfies

$$\hat{L}_{ij,\tau} = \begin{cases} L_{ij} v_{\tau, \tau_{j,i}}, & \text{if } i \neq j \\ L_{ii} v_{\tau, \tau_{j,i}}, & \text{if } i = j \end{cases} \quad (13)$$

According to this definition, we have  $\sum_{\tau=0}^{\tau_m} \hat{L}_\tau = L$ .

$$\Phi(t) = \begin{bmatrix} \bar{A}(t) & -(\hat{L}_0(t) + I_0(t)) \otimes \sigma BK & \dots & -(\hat{L}_{\tau_{m-1}}(t) + I_{\tau_{m-1}}(t)) \otimes \sigma BK \\ I_N \otimes I_n & 0 & \dots & 0 \\ \vdots & \ddots & \dots & \vdots \\ 0 & \dots & I_N \otimes I_n & 0 \end{bmatrix} \quad (14)$$

To help analyze the stability of the system, we introduce a matrix

$$\theta = \begin{bmatrix} y_{10} & y_{11} & \dots & y_{1\tau_m} \\ I_N \otimes I_n & 0 & \dots & 0 \\ \vdots & \ddots & \dots & \vdots \\ 0 & \dots & I_N \otimes I_n & 0 \end{bmatrix} \quad (15)$$

where  $y_{1j}$  is a sub-matrix and  $j = 0, 1, \dots, \tau_m$ . Let  $\theta_{i,j}^n$  denote the element of the  $i$ th row and the  $j$ th column of the matrix  $\theta^n$ . Lemma 2 is then presented to specify the convergence condition of  $\theta$ .

**Lemma 2.**  $\theta$  is a convergence matrix, if there is an appropriate  $\tau_m$  such that  $\lim_{n \rightarrow \infty} \|\theta_{1,1}^n\|_{\infty} = 0$ .

*Proof.* By the definition of  $\theta$ , we have

$$\begin{cases} \theta_{i,1}^n = y_{10}\theta_{i,1}^{n-1} + \theta_{i,2}^{n-1} \\ \theta_{i,k}^n = y_{1k-1}\theta_{i,1}^{n-1} + \theta_{i,k}^{n-1} \\ \theta_{i,\tau_m}^n = y_{i\tau_m}\theta_{i,1}^{n-1} \end{cases} \quad (16)$$

where  $n \geq 2$ ,  $i = 1$  and  $k$  is a positive integer satisfying  $1 \leq k \leq \tau_m - 1$ . Further, when  $2 \leq i \leq \tau_m$ , we can obtain

$$\theta_{i,k}^n = \theta_{i-1,k}^{n-1} \quad (17)$$

By analyzing the above iterative Eq. (16) (17), we know if  $\lim_{t \rightarrow \infty} \|\theta_{1,1}^t\|_{\infty} = 0$ , we have  $\lim_{t \rightarrow \infty} \|\theta_{1,1}^{t-1}\|_{\infty} = 0$ , which leads to  $\lim_{t \rightarrow \infty} \|\theta_{1,2}^{t-1}\|_{\infty} = 0$ . This result further supports  $\lim_{t \rightarrow \infty} \|\theta_{1,k}^{t-1}\|_{\infty} = 0$  and  $\lim_{t \rightarrow \infty} \|\theta_{i,k}^t\|_{\infty} = 0$ . Finally, we have  $\lim_{t \rightarrow \infty} \theta^t = 0$ .  $\square$

Since we know  $\delta_i(t) = \xi_i(t) - f_i(t)$ , we have  $\delta_i(t - \tau) = \xi_i(t - \tau) - f_i(t)$ . If  $\tau = 0$ , they are equivalent. The settings of feedback matrices  $K_1$  and  $K_2$  are the same as before and we have  $K = K_2 = -K_1$ . Therefore,  $\delta(t)$  can be written as

$$\delta(t+1) = \tilde{A}\delta(t) - \sum_{l=0}^{\tau_{m-1}} ((\hat{L}_l(t) + I_l(t)) \otimes \sigma BK) \delta(t-l) \quad (18)$$

where  $I_l$  is a diagonal matrix with the element being  $I_{l,ii} = I_{ii} \nu_{\tau, \tau_{i,i}}$ , satisfying  $\sum_{l=0}^{\tau_m} I_l = I_N$ .

To further simplify system analysis, we denote  $\tilde{\delta}(t) = [\delta^T(t), \delta^T(t-1), \dots, \delta^T(t-\tau_m)]^T$ . Then, we can further rewrite Eq. (18) as

$$\tilde{\delta}(t+1) = \Phi(t)\tilde{\delta}(t) \quad (19)$$

where  $\Phi(t)$  is the system error matrix with  $\bar{A} = \tilde{A} - (\hat{L}_0(t) + I_0(t)) \otimes \sigma BK$ . Let  $\Phi_{i,j}$  be the  $i$ th row and  $j$ th column of  $\Phi$ .

The matrix  $\Phi(t)$  is a full-rank matrix, so it is a diagonalizable matrix. Similarly, let  $\tilde{h}(t) = (\tilde{v}_1 \otimes I_n)\tilde{\delta}(t)$  and  $\tilde{\delta}(t) = (\tilde{V} \otimes I_n)\tilde{\delta}(t)$ . Then, we can define  $\hat{h}(t) = (V \otimes I_n)[\tilde{h}(t), 0]^T$  and  $\hat{\delta}(t) = (V \otimes I_n)[0, \tilde{\delta}(t)]^T$ . Then, we also get  $\delta(t) = \hat{h}(t) + \hat{\delta}(t)$ . let  $\hat{\delta}(t) = \delta(t) - \hat{h}(t)$  and we know  $h(t)$  exist. Similarly, we can prove the convergence of  $\hat{h}(t)$  to illustrate the feasibility of the time-varying formation. Because  $\|\hat{\delta}(t)\| = \|\tilde{\delta}(t)\| = \|\tilde{\delta}(t)\|$ , we only need to consider  $\tilde{\delta}(t)$ .

The following theorem ensures that the intended formation with varying delays can be achievable under the formation controller (12).

**Theorem 2.** For any multi-UAV systems under the designed formation control protocol (7), if  $0 < k_1, k_2 < 1$  and  $\sigma k_1 < k_2 < \frac{4k_1}{\lambda_N(\mathcal{G})+1}$  are satisfied, and  $\lim_{n \rightarrow \infty} \|\Phi_{1,1}^n\|_{\infty} = 0$  with allowable  $\tau_m$  is met, the time-varying formation  $F(t)$  can be achieved under time-varying topologies and delay.

*Proof.* Considering the definition of  $\tilde{\delta}(t)$ , if  $\tilde{\delta}(t)$  is convergent, we know the formation error  $\delta(t)$  converges. Thus, we need to prove the convergence of  $\Phi(t)$ .

Here,  $\theta$  is equal to  $\Phi(t)$  if

$$\begin{cases} y_{11} = \bar{A}(t) \\ y_{12} = -(\hat{L}_1(t) + I_1(t)) \\ \dots \\ y_{1\tau_m} = -(\hat{L}_{\tau_m}(t) + I_{\tau_m}(t)) \otimes \sigma BK \end{cases} \quad (20)$$

According to Lemma 2, if  $\lim_{n \rightarrow \infty} \|\Phi_{1,1}^n\|_{\infty} = 0$  is satisfied,  $\Phi(t)$  is a convergent matrix. According to Theorem 1, we know that if  $0 < k_1, k_2 < 1$  and  $\sigma k_1 < k_2 < \frac{4k_1}{\lambda_N(\mathcal{G})+1}$  are satisfied and there is an appropriate  $\tau_m$ , we have  $\lim_{n \rightarrow \infty} \|\Phi_{1,1}^n\|_{\infty} = 0$ .

Then, we can conclude that  $\tilde{\delta}(t)$  is convergent. Because  $\delta(t)$  is one of the elements of  $\tilde{\delta}(t)$ , we can say  $\delta(t)$  is convergent. Therefore, the multi-UAV system can achieve the anticipated formation within the allowable range of error. The above Theorem 2 holds.  $\square$

Theorem 2 reveals that to ensure the stability of the system, we should guarantee the delay in each connected channel is less than  $t_m$ , which is associated with the number of connected channels and the number of UAVs if  $\sigma, k_1$  and  $k_2$  follow Theorem 1.

Given Theorem 2, the key is to find the appropriate  $\tau_m$ . Here we present *Algorithm 1* to obtain  $\tau_m$ . The value of  $n$  is obtained from experiments.

Algorithm 1 computes the infinity norm of the system matrix  $\Phi(t)$  through numerical analysis methods. The goal is

**Algorithm 1** Algorithm for obtaining  $\tau_m$  allowed by the system

---

```

1: function
2:   Initialize  $\tau_m = 0, n = 50, T = 0$ 
3:   while  $\tau_m \geq 0$  do
4:      $T = T + 1$ 
5:     for  $i=1:n$  do
6:       Randomly select the connected channels in
7:       the channel set  $\mathcal{E}$ ; Randomly select the delay
8:       for each connected channel in set  $\{0, \dots, \tau_m\}$ .
9:       Calculate  $\Phi_{1,1}^i, \Phi_{1,1}^{i+1}$ :  $\Phi_{1,1}^i = \bar{A}(t)\Phi_{1,1}^{i-1} + \Phi_{1,2}^{i-1}$ ,
10:       $\Phi_{1,1}^{i+1} = \bar{A}(t)\Phi_{1,1}^i + \Phi_{1,2}^i$ 
11:     end for
12:     if  $\|\Phi_{1,1}^{n+1}\|_\infty < \|\Phi_{1,1}^n\|_\infty$  then
13:       if  $T == 1$  then
14:          $\tau_m = \tau_m + 1, T = 0$ 
15:       else
16:         Break
17:       end if
18:     else
19:        $\tau_m = \tau_m - 1$ 
20:     end if
21:   end while
22:   return  $\tau_m$ 
23: end function

```

---

to find the maximum time delay  $\tau_m$  that satisfies the conditions for the convergence of the system matrix.

According to Algorithm 1, as  $\tau_m = \lceil \frac{t_m}{\sigma} \rceil$ , a relatively small  $\sigma$  can tolerate a larger  $\tau_m$ , but the convergence speed will decrease with a larger  $\tau_m$ , because it takes more time steps to make  $\|\Phi(t)\|^t < 1$  if  $\tau_m$  increases according to Eq. (16). Therefore, there is a trade-off between  $\tau_m$  and the system convergence speed.

Since the special form of the Laplacian matrix  $\hat{L}_{ij,\tau}$  includes both internal and external delay, it is very difficult to analyze their impact on the system in isolation, but we can study the extreme cases to help learn it. We assume that one of them is zero, and then we can use Algorithm 1 to compute  $\tau_m$ . The result shows the system can allow larger external delay and is more sensitive to internal delay. The internal delay has a bigger impact on the stability of the system.

### C. The deployment of multi-UAV systems with time-varying delays

In most practical application scenarios (e.g. agricultural UAVs, search and rescue, edge computing UAV, delivery), UAVs will spread in large areas. Generally, there are two cases: 1) UAVs go to different positions; 2) some UAVs go to the same position in the formation and others go to different positions separately. Here we assume that we have got the trajectories  $h(t)$  of each UAV generated between the start point and destination according to some through some trajectory generation algorithms [35]. If we want to make multiple UAVs

follow a specific trajectory, the formation controller becomes:

$$u_i(t) = K_1 (\xi_i(t) - f_i(t) - h_i(t)) + \kappa \cdot \Delta h_{iv}(t) + K_2 \sum_{j=1}^N w_{ij}(t) ((\xi_j(t) - f_j(t)) - (\xi_i(t) - f_i(t))) \quad (21)$$

where  $\Delta h_{iv}(t) = [\Delta h_{iv_1}(t), \dots, \Delta h_{iv_n}(t)]^T$  with  $\Delta h_{iv_n}(t) = h_{iv_n}(t+1) - h_{iv_n}(t)$ , and  $\kappa = \frac{1}{\sigma}$ .

For case 1, since each UAV focuses on its own trajectory, there is no communication link in this process. Then, the controller becomes

$$u_i(t) = K_1 (\xi_i(t - \tau_{i,i}(t)) - f_i(t) - h(t - \tau_{i,i}(t))) + \kappa \cdot \Delta h_v(t) \quad (22)$$

It is a special case of the controller (12) when  $w_{ij}(t) = 0$ , so these parameters are the same as the above controller (12) and the system convergence can be ensured. Differently, we have  $f_i = 0$  in the process of UAV deployment, and  $h_i(t)$  is adjusted according to target points  $(p_{ix}, p_{iy}, p_{iz})$  of the  $i$ th UAV. For example, we can set  $h_i(t) = v_{ix}t_s + v_{iy}t_s + v_{iz}t_s$ , where  $v_{ix}$ ,  $v_{iy}$  and  $v_{iz}$  represent velocity in X, Y and Z dimensions, respectively. Let  $\frac{p_{ix}}{v_{ix}} = \frac{p_{iy}}{v_{iy}} = \frac{p_{iz}}{v_{iz}}$ . We have  $t_s = t$  if  $t \leq \frac{p_{ix}}{v_{ix}}$  and  $t_s = 0$  if  $t > \frac{p_{ix}}{v_{ix}}$ .

For case 2, the controller is the same as the controller (12). Different from the first case, if the  $i$ th,  $j$ th and  $m$ th UAV need to fly to the same location in formation, then the parameters of  $f_i$ ,  $f_j$  and  $f_m$  should be the formation of the three UAVs and  $h_i = h_j = h_m$  holds. For other UAVs that fly alone, the setting is the same as the first case.

## IV. EXPERIMENTS

We provide simulation experiments and hardware experiments to evaluate the theoretical results. Here we choose four UAVs, labelled  $\{1, 2, 3, 4\}$  in the three-dimensional space for simulation. Similar experiments can be carried out using different settings such as different numbers of UAVs, varied initial network connections, and other formation shapes. We design time-varying formation as  $f_i(t) = [5\sigma \sin(t\pi/24 + (i-1)\pi/2), 5\sin(t\pi/24 + (i-1)\pi/2) - 5\sin((t-1)\pi/24 + (i-1)\pi/2), 5\sigma \cos(t\pi/24 + (i-1)\pi/2), 5\cos(t\pi/24 + (i-1)\pi/2) - 5\cos((t-1)\pi/24 + (i-1)\pi/2), 0, 0]^T$ , from which we can see that the four UAVs will continually form circular formations. Let  $\sigma = 0.2$ . Considering Theorem 1 and Theorem 2, we get  $K = I_3 \otimes [0.08, 0.13]$  that concurrently satisfies the conditions stipulated in Theorem 1 and Theorem 2. According to Algorithm 1, we get the maximum delay allowed by this system is  $\tau_m = 2$ . The parameters are used in all the experiments in this paper.

The basic network topology is shown in Fig. 1, where each solid line represents the links between UAVs. In order to simulate the scenario where some channels may fail at a certain time, every link at each time step is alive with a probability  $p \geq 0.7$  and fails with a probability  $1 - p$ . For fixed topology, the solid line is always connected.

We initially present the simulation results of multiple UAVs forming time-varying formations under a fixed topology that is a connected graph, as shown in Fig. 2. The corresponding input of the controller is given in Fig. 3.

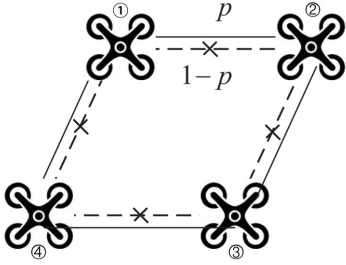


Fig. 1. The time-varying topologies.

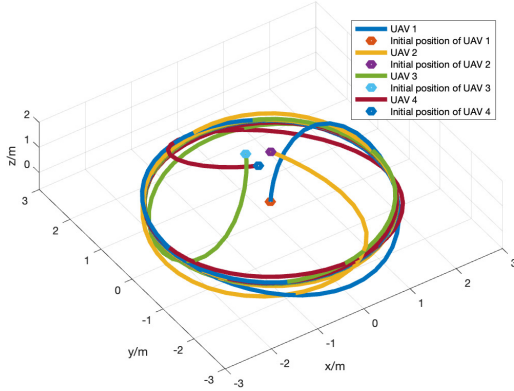


Fig. 2. The process of achieving time-varying formation under fixed topology.

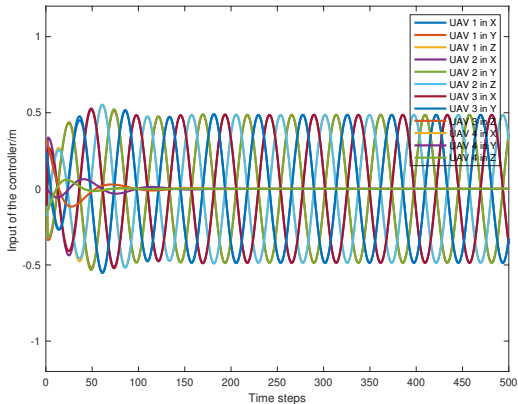


Fig. 3. The change of the input of the controller under fixed topology.

#### A. Multi-UAV networks with changing topologies

Then we explore the performance of our method with dynamic topologies. Fig. 4 shows the connection status of all links in the first 50 time steps. In this figure, if the link (1,2) is at its high level, there exists a connection between the 1st UAV and the 2nd UAV. If the link (1,4) is at its high level, the 1st UAV establish a connection with the 4th UAV. Similarly, when (2,3) and (3,4) are at their high level, we have the corresponding connection between the 2nd UAV and 3rd UAV and between the 3rd UAV and the 4th UAV. With this, we can learn about how the topology is changing in this experiment. Here we adopt the reciprocal setting that (x, y)

denotes the two-way channel between x and y.

Fig. 5 illustrates the formation process, where the time-varying formation is eventually achieved in three dimensions and each curve represents the trajectory of a UAV in one dimension (X, Y or Z). The change of the control input  $u_i$  is shown in Fig. 6. Compared to Fig. 3, the curve in Fig. 6 appears to be more rugged and less smooth because of the changing topologies.

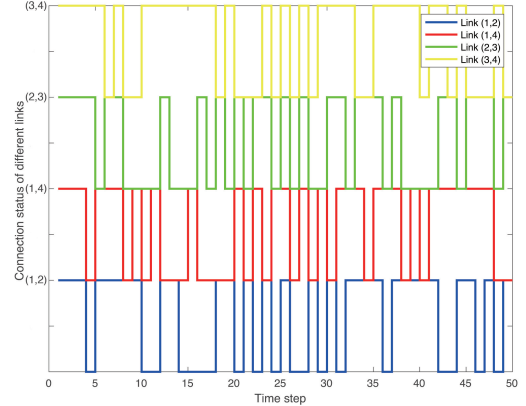


Fig. 4. The connection status of different links in 50 time steps.

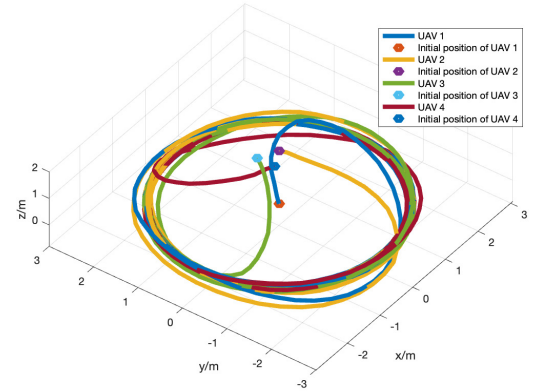


Fig. 5. The process of achieving time-varying formation under changing topologies.

#### B. Multi-UAV networks with changing topologies and time-varying communication delay

The next experiment studies the scenario with time-varying delays. The channel is still unstable, the same as in previous settings. The delay  $\tau(t)$  at each time step is random but satisfies  $\tau(t) \leq \tau_m$ . According to Algorithm 1, we input the basic settings of this system and get  $\tau_m = 2$ . Then we have the real delay  $t_m = \sigma\tau_m = 0.4s$  that can be applied to the actual situation because it is greater than the delay in many real systems [31].

When  $\tau_m = 2$ , Fig. 7 displays the position of UAVs in three dimensions during formation, where the circular formation

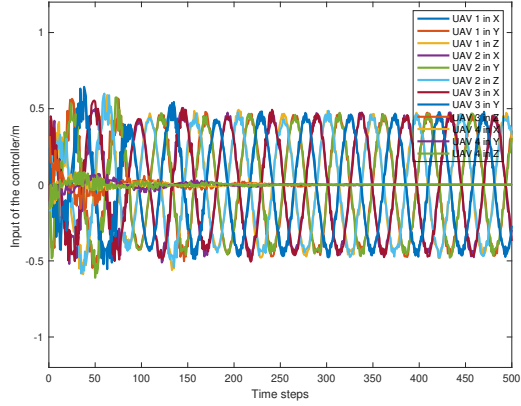


Fig. 6. The control input under dynamics topologies.

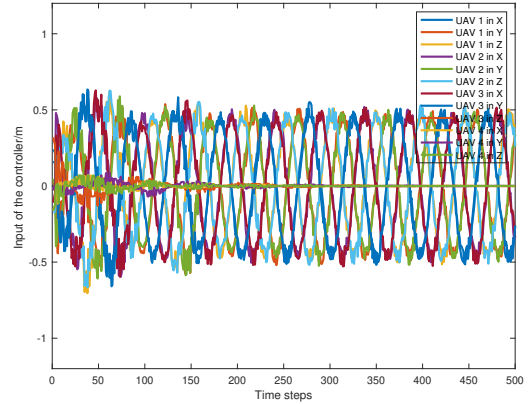


Fig. 8. The control input when  $\tau_m = 2$ .

is not as smooth as the previous one in Fig. 5, due to the effects of time delay and dynamic topology. From Fig 8, the corresponding control input no longer exhibits standard oscillations, but the range of the input values remains bounded. Fig. 9 shows the acceptable formation error of one UAV, where each line represents the formation error in one dimension.

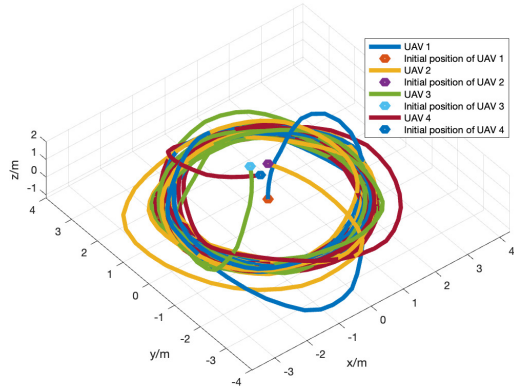


Fig. 7. The process of achieving time-varying formation when  $\tau_m = 2$ .

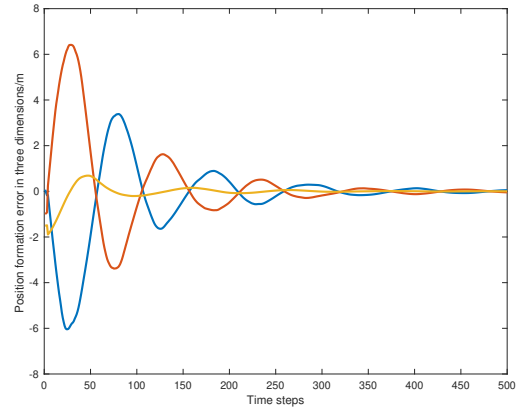


Fig. 9. The formation error with  $\tau_m = 2$ .

When  $\tau_m = 3$  that is greater than the maximum delay allowed by the system, Fig. 10 confirms that the UAVs cannot achieve the desired formation, where the flight of the UAVs is very chaotic. In Fig. 11, we can further see that the formation error is large in this case.

### C. The deployment of multi-UAV systems with time-varying delays

In this experiment, we will deploy 4 UAVs labelled 1, 2, 3, 4 to targets. The parameters  $\sigma$ ,  $k_1$  and  $k_2$  are the same as the previous settings. Let  $\tau_m = 2$ .

For case 1, four targets are set as  $O_1(10, 0)$ ,  $O_2(25, 8.66)$ ,  $O_3(25, -8.66)$  and  $O_4(0, 0)$  in the object area, which can be set according to actual needs. Then we initiate each UAV's velocity, which is  $v_1 = [0.2, 0, 0]^T$ ,  $v_2 = [0.5, 0.1732, 0]^T$ ,  $v_3 = [0.5, -0.1732, 0]^T$  and  $v_4 = [0, 0, 0]^T$ , respectively. Then

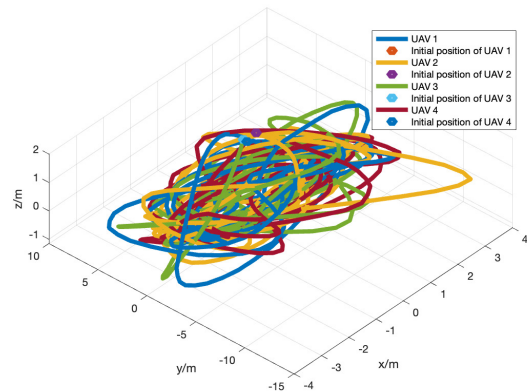


Fig. 10. The process of achieving time-varying formation when  $\tau_m = 3$ .

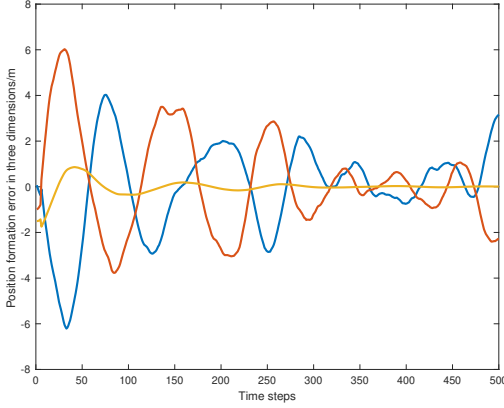


Fig. 11. The formation error with  $\tau_m = 3$ .

under the controller (21), UAVs can reach the different targets as shown in Fig. 12, where the coordinates of the final points of UAVs have been marked.

For case 2, we assume every two UAVs (UAV 1 and UAV 2, UAV 3 and UAV 4) will maintain a formation to fly to the target points. The communication channels in the two groups are randomly connected or disconnected. The target points of UAVs are set as  $O_1(25, 8.66)$ ,  $O_2(20.5278, 10.8961)$ ,  $O_3(25, -8.66)$  and  $O_4(20.5278, -10.8961)$ . We design the line formation for them as  $f_1 = [0, 0, 0, 0, 0]^T$ ,  $f_2 = [-4.4722, 0, 2.2361, 0, 0]^T$ ,  $f_3 = [0, 0, 0, 0, 0]^T$ ,  $f_4 = [-4.4722, 0, -2.2361, 0, 0]^T$ . The initial position of 4 UAVs can be random. Fig. 13 shows that all UAVs have reached the target points within the allowable error bound.

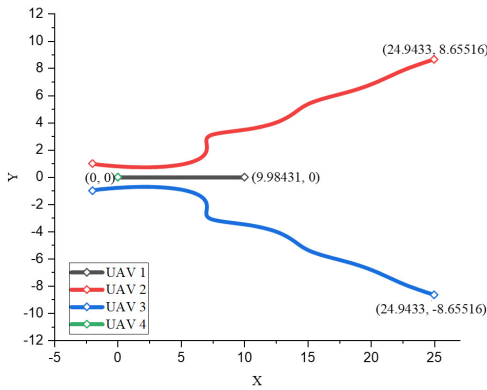


Fig. 12. Four UAVs go to different points.

#### D. Hardware experiments for multi-UAV systems

The following hardware experiments are conducted to verify the feasibility of the designed flight pattern proposed by our formation algorithm. To implement this UAV formation hardware experiment, we have considered multiple aspects, including size, accuracy, and wireless connectivity. We chose Crazyflie because it is easy to configure and has the required

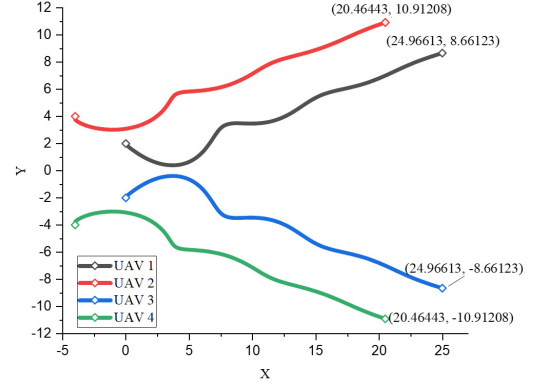


Fig. 13. The UAV formation is divided into two sub-formations, which fly to the target point respectively.

performance metrics, including high accuracy. Furthermore, it weighs 27g and is safe for swarm experiments, particularly in indoor scenarios. For these reasons, it is also a widely used platform for academic research on multiple UAVs. Two base stations (Lighthouse 1 and Lighthouse 2) are placed in different corners of the room and they emit infrared light. The infrared light is structured in a pattern that sweeps across the room. Then, The Crazyflie drone is equipped with sensors that can detect this light. By analyzing the timing and pattern of the received light, the Crazyflie can calculate its position through this lighthouse positioning system.

The flow chart of this hardware experiment is given in Fig. 14. It mainly includes two parts: 1) The Lighthouse positioning system provides accurate positioning data; 2) Our method calculates the required movements. Then, the four 'Crazyflie 2.1' can achieve the time-varying formation based on these data.

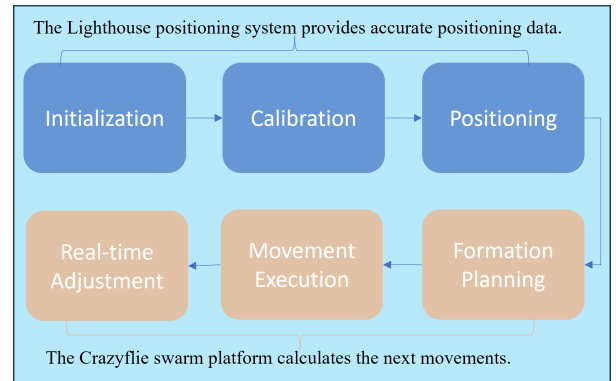


Fig. 14. The flow chart of hardware experiment using Lighthouse positioning system.

A computer installed on Ubuntu 20.04 is used to compute the trajectories of UAVs based on the controller with delay. And a crazy radio plugged into the computer is used to transmit the generated trajectories to UAVs (Crazyflie 2.1). Four UAVs are chosen, which is consistent with the setting of the simulation experiment.

Due to the limited indoor experimental space, we reduced the size of the desired formation to one-twentieth of the simulated formation. The system parameters including the system control gain  $\sigma$ , the system feedback matrix  $K$  and  $\tau_m$  are the same as simulation experiments. The size of the physical map is  $2m \times 2m$ . Initially, four UAVs are put at random. Fig.15 (a)-(d) shows the process of formation, from which we can see no collision happens among UAVs and the time-varying circular formation is effectively reached in hardware. The whole process of formation can be more clearly seen in the online video (<https://www.youtube.com/watch?v=7bfICVWNfXc>). Fig. 16 shows the physical trajectory error between the expected trajectory and the real trajectory. From the figure, we can see that the physical trajectory error is within 5cm, which results from the error of our deployment positioning system. Since our Lighthouse positioning system is an optical system, the accuracy of this system will be better if we put the Lighthouse base stations higher so that Lighthouse base stations can cover the experiment area better.

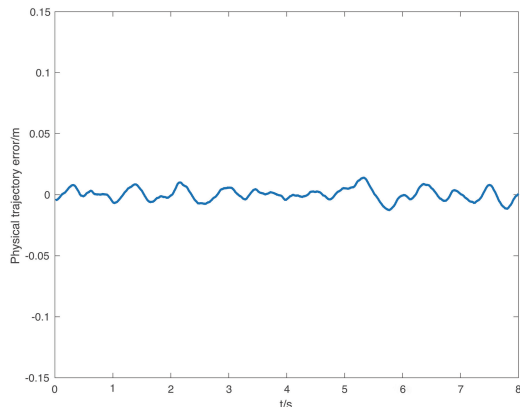
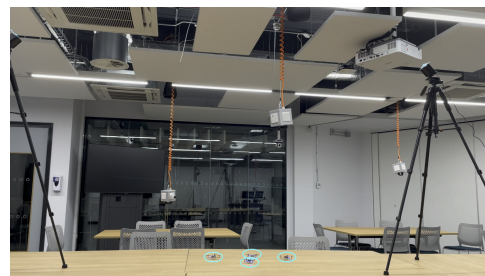


Fig. 16. The physical trajectory error between the expected trajectory and the real trajectory.

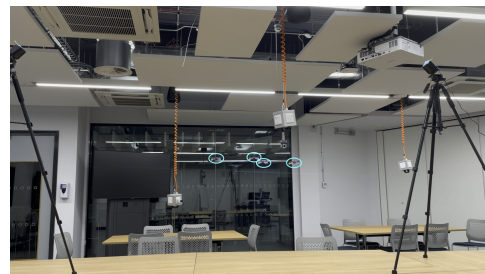
## V. CONCLUSIONS

In this paper, we proposed the time-varying formation algorithm for multi-UAV systems with time-varying topologies and hybrid delays. Based on the state information from the UAV itself and neighbours, the distributed control protocols could steer UAVs to fly in the time-varying formation and achieve the deployment of UAVs. We gave sufficient conditions for formation in different scenarios with or without delays and proved the system convergence. An algorithm was provided to obtain the maximum delay allowed by the system. Numerical experiments and UAV hardware experiments were conducted to evaluate the performance of the theoretical results and the feasibility of this flight pattern.

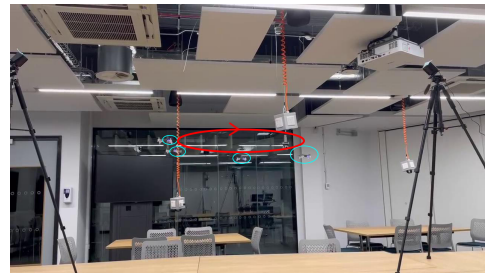
In future research, it is worth considering the impact of interference and delays on large-scale multi-UAV systems to improve the robustness of such a system. Furthermore, modelling and analyzing large-scale systems with uncertain nonlinear factors remain challenging.



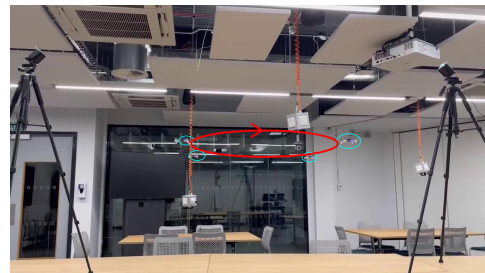
(a)



(b)



(c)



(d)

Fig. 15. Four UAVs achieve the time-varying formation in 'Crazyflie 2.1 platform' (a) The initial position. (b) UAVs are adjusting their positions to form the formation. (c) The UAVs continue forming the circular formation. (d) The UAVs continue forming the time-varying circular formation.

## VI. ACKNOWLEDGMENT

This work was partly supported by the EU Horizon 2020 Research and Innovation Programme under the Marie Skłodowska-Curie grant agreement No 101008297. This article reflects only the authors' view. The European Union Commission is not responsible for any use that may be made of the information it contains. This work was partially supported by the Royal Society (Grant No. IEC\NSFC\223418).

## REFERENCES

- [1] B. P. Tice, "Unmanned aerial vehicles: The force multiplier of the 1990s," *Airpower Journal*, vol. 5, no. 1, pp. 41–55, 1991.
- [2] N. Delavarpour, C. Koparan, Y. Zhang, D. D. Steele, K. Betitame, S. G. Bajwa, and X. Sun, "A review of the current unmanned aerial vehicle sprayer applications in precision agriculture," *Journal of the ASABE*, p. 0, 2023.
- [3] Y.-H. Ho and Y.-J. Tsai, "Open collaborative platform for multi-drones to support search and rescue operations," *Drones*, vol. 6, no. 5, p. 132, 2022.
- [4] T. Nguyen, R. Katila, and T. N. Gia, "An advanced internet-of-drones system with blockchain for improving quality of service of search and rescue: A feasibility study," *Future Generation Computer Systems*, vol. 140, pp. 36–52, 2023.
- [5] P. McEnroe, S. Wang, and M. Liyanage, "A survey on the convergence of edge computing and ai for uavs: Opportunities and challenges," *IEEE Internet of Things Journal*, vol. 9, no. 17, pp. 15435–15459, 2022.
- [6] V. R. Miranda, A. M. Rezende, T. L. Rocha, H. Azpúrua, L. C. Pimenta, and G. M. Freitas, "Autonomous navigation system for a delivery drone," *Journal of Control, Automation and Electrical Systems*, vol. 33, pp. 141–155, 2022.
- [7] Y. Wu, S. Xu, W. Dai, and L. Lin, "Heuristic position allocation methods for forming multiple uav formations," *Engineering Applications of Artificial Intelligence*, vol. 118, p. 105654, 2023.
- [8] J. Duan, G. Duan, S. Cheng, S. Cao, and G. Wang, "Fixed-time time-varying output formation–containment control of heterogeneous general multi-agent systems," *ISA transactions*, vol. 137, pp. 210–221, 2023.
- [9] N. A. Thuyen, P. N. N. Thanh, and H. P. H. Anh, "Adaptive finite-time leader-follower formation control for multiple auvs regarding uncertain dynamics and disturbances," *Ocean Engineering*, vol. 269, p. 113503, 2023.
- [10] S. I. Azid, K. Raghuvaiya, A. Javed, and E. Kumari, "Autonomous leader–follower formation of vehicular robots using the lyapunov method," *Unmanned Systems*, vol. 12, no. 01, pp. 75–85, 2024.
- [11] C. Wei, X. Wu, B. Xiao, J. Wu, and C. Zhang, "Adaptive leader-following performance guaranteed formation control for multiple spacecraft with collision avoidance and connectivity assurance," *Aerospace Science and Technology*, vol. 120, p. 107266, 2022.
- [12] S. Moorthy and Y. H. Joo, "Distributed leader-following formation control for multiple nonholonomic mobile robots via bioinspired neurodynamic approach," *Neurocomputing*, vol. 492, pp. 308–321, 2022.
- [13] G. Vásárhelyi, C. Virágh, G. Somorjai, T. Nepusz, A. E. Eiben, and T. Vicsek, "Optimized flocking of autonomous drones in confined environments," *Science Robotics*, vol. 3, no. 20, p. eaat3536, 2018.
- [14] C. Gao, J. Ma, T. Li, and Y. Shen, "Hybrid swarm intelligent algorithm for multi-uav formation reconfiguration," *Complex & Intelligent Systems*, pp. 1–34, 2022.
- [15] S. Shao, Y. Peng, C. He, and Y. Du, "Efficient path planning for uav formation via comprehensively improved particle swarm optimization," *ISA transactions*, vol. 97, pp. 415–430, 2020.
- [16] W. Cheng, K. Zhang, and B. Jiang, "Continuous fixed-time fault-tolerant formation control for heterogeneous multiagent systems under fixed and switching topologies," *IEEE Transactions on Vehicular Technology*, 2022.
- [17] D. Zhang and H. Duan, "Switching topology approach for uav formation based on binary-tree network," *Journal of the Franklin Institute*, vol. 356, no. 2, pp. 835–859, 2019.
- [18] J. Gong, Y. Ma, B. Jiang, and Z. Mao, "Distributed adaptive fault-tolerant formation control for heterogeneous multiagent systems under switching directed topologies," *Journal of the Franklin Institute*, vol. 359, no. 8, pp. 3366–3388, 2022.
- [19] J. Wu, C. Luo, Y. Luo, and K. Li, "Distributed uav swarm formation and collision avoidance strategies over fixed and switching topologies," *IEEE Transactions on Cybernetics*, vol. 52, no. 10, pp. 10969–10979, 2021.
- [20] H. J. Savino, C. R. dos Santos, F. O. Souza, L. C. Pimenta, M. de Oliveira, and R. M. Palhares, "Conditions for consensus of multi-agent systems with time-delays and uncertain switching topology," *IEEE Transactions on Industrial Electronics*, vol. 63, no. 2, pp. 1258–1267, 2015.
- [21] R. Olfati-Saber and R. M. Murray, "Consensus problems in networks of agents with switching topology and time-delays," *IEEE Transactions on automatic control*, vol. 49, no. 9, pp. 1520–1533, 2004.
- [22] J. Qin, H. Gao, and W. X. Zheng, "Second-order consensus for multi-agent systems with switching topology and communication delay," *Systems & Control Letters*, vol. 60, no. 6, pp. 390–397, 2011.
- [23] Z. Wang, J. Xu, and H. Zhang, "Consensusability of multi-agent systems with time-varying communication delay," *Systems & Control Letters*, vol. 65, pp. 37–42, 2014.
- [24] S. Liu, L. Xie, and H. Zhang, "Distributed consensus for multi-agent systems with delays and noises in transmission channels," *Automatica*, vol. 47, no. 5, pp. 920–934, 2011.
- [25] Z. Yan, L. Han, X. Li, X. Dong, Q. Li, and Z. Ren, "Event-triggered formation control for time-delayed discrete-time multi-agent system applied to multi-uav formation flying," *Journal of the Franklin Institute*, vol. 360, no. 5, pp. 3677–3699, 2023.
- [26] V. Sharma, K. Srinivasan, H.-C. Chao, K.-L. Hua, and W.-H. Cheng, "Intelligent deployment of uavs in 5g heterogeneous communication environment for improved coverage," *Journal of Network and Computer Applications*, vol. 85, pp. 94–105, 2017.
- [27] R. Masroor, M. Naeem, and W. Ejaz, "Efficient deployment of uavs for disaster management: a multi-criterion optimization approach," *Computer Communications*, vol. 177, pp. 185–194, 2021.
- [28] Y. Kang, D. Luo, B. Xin, J. Cheng, T. Yang, and S. Zhou, "Robust leaderless time-varying formation control for nonlinear unmanned aerial vehicle swarm system with communication delays," *IEEE Transactions on Cybernetics*, 2022.
- [29] J. Wang, L. Han, X. Li, X. Dong, Q. Li, and Z. Ren, "Time-varying formation of second-order discrete-time multi-agent systems under non-uniform communication delays and switching topology with application to uav formation flying," *IET Control Theory & Applications*, vol. 14, no. 14, pp. 1947–1956, 2020.
- [30] Z. Wang, M. Xu, L. Liu, C. Fang, Y. Sun, and H. Chen, "Optimal uav formation tracking control with dynamic leading velocity and network-induced delays," *Entropy*, vol. 24, no. 2, p. 305, 2022.
- [31] A. Garcia-Santiago, J. Castaneda-Camacho, J. F. Guerrero-Castellanos, and G. Mino-Aguilar, "Evaluation of aodv and dsdv routing protocols for a fanet: Further results towards robotic vehicle networks," in *2018 IEEE 9th Latin American Symposium on Circuits & Systems (LASCAS)*, pp. 1–4, IEEE, 2018.
- [32] C. Ma and J. Zhang, "On formability of linear continuous-time multi-agent systems," *Journal of Systems Science and Complexity*, vol. 25, no. 1, pp. 13–29, 2012.
- [33] X. Dong, B. Yu, Z. Shi, and Y. Zhong, "Time-varying formation control for unmanned aerial vehicles: Theories and applications," *IEEE Transactions on Control Systems Technology*, vol. 23, no. 1, pp. 340–348, 2014.
- [34] R. Merris, "A note on laplacian graph eigenvalues," *Linear algebra and its applications*, vol. 285, no. 1-3, pp. 33–35, 1998.
- [35] K. Raigoza and T. Sands, "Autonomous trajectory generation comparison for de-orbiting with multiple collision avoidance," *Sensors*, vol. 22, no. 18, p. 7066, 2022.



**Jia Wu** received the B.E. degree from Southwest University, Chongqing, China, in 2018, and the M.E. degree from the University of Electronic Science and Technology of China, Chengdu, China, in 2021. She is currently pursuing the Ph.D. degree with the Department of Computer Science, Faculty of Environment, Science and Economy, University of Exeter, Exeter, U.K. Her research interests mainly include distributed multiagent systems, UAVs control and mobile edge computing.



**Chunbo Luo** received the Ph.D. degree in high performance cooperative wireless networks from the University of Reading, Reading, U.K., in 2011. His research interest focuses on developing model-based and machine learning algorithms to solve networking and engineering problems, such as wireless networks, with a particular focus on unmanned aerial vehicles.



Modelling and Performance Engineering.

**Geyong Min** is a Professor of High Performance Computing and Networking in the Department of Computer Science at the University of Exeter, United Kingdom. He received the PhD degree in Computing Science from the University of Glasgow, United Kingdom, in 2003, and the B.Sc. degree in Computer Science from Huazhong University of Science and Technology, China, in 1995. His research interests include Computer Networks, Wireless Communications, Parallel and Distributed Computing, Ubiquitous Computing, Multimedia Systems,



**Sally McClean** Sally McClean received her first degree in Mathematics from Oxford University, and then obtained a MSc in Mathematical Statistics and Operational Research from Cardiff University, followed by a PhD on Markov and semi-Markov models at Ulster University. She is currently Professor of Mathematics at Ulster University. Her main research interests are in Stochastic Modelling and Optimisation, particularly for Healthcare Planning, and Computer Science, specifically Databases, Process Mining, Sensor Technology and Telecommunications. Much of this work has been focussed on healthcare and business applications, particularly with regard to patient or customer modelling and pervasive technologies. More recently she has been working in the Invest Northern Ireland (INI) funded Ireland Innovation Centre (BTIIC) mainly carrying out research into Process Modelling and Mining and was the UU Principal Investigator for several years.